Synthesis, Structures, and Electrochemistry of Palladium and Platinum Macrocyclic Complexes of [18]aneN$_2$S$_4$ (1,4,10,13-Tetrathia-7,16-diazacyclo-octadecane) and Me$_2$[18]aneN$_2$S$_4$ (7,16-Dimethyl-1,4,10,13-tetrathia-7,16-diazacyclo-octadecane). Single Crystal *X*-Ray Structures of [Pd(Me$_2$[18]aneN$_2$S$_4$)][PF$_6$]$_2$·Me$_2$CO, [Pd([18]aneN$_2$S$_4$)][BPh$_4$]$_2$, and [Pd$_2$Cl$_2$([18]aneN$_2$S$_4$)][PF$_6$]$_2$·2MeCN†

Alexander J. Blake, Gillian Reid and Martin Schröder*
Department of Chemistry, University of Edinburgh, West Mains Road, Edinburgh EH9 3JJ, Scotland

Reaction of PdCl$_2$ with the N$_2$S$_4$ donor macrocycles [18]aneN$_2$S$_4$ (1,4,10,13-tetrathia-7,16-diazacyclo-octadecane) and Me$_2$[18]aneN$_2$S$_4$ (7,16-dimethyl-1,4,10,13-tetrathia-7,16-diazacyclo-octadecane) affords the 1:1 complex cations [Pd([18]aneN$_2$S$_4$)]$^{2+}$ and [Pd(Me$_2$[18]aneN$_2$S$_4$)]$^{2+}$ respectively in high yield. The yellow complex [Pd(Me$_2$[18]aneN$_2$S$_4$)][PF$_6$]$_2$·Me$_2$CO crystallises in the orthorhombic space group *Pcab*, with a = 14.3369(15), b = 17.691 5(7), c = 24.295 2(11) Å, and Z = 8. The single crystal *X*-ray structure of [Pd(Me$_2$[18]aneN$_2$S$_4$)]$^{2+}$ shows square-planar co-ordination at Pd^{II} with the four thioether donors of the macrocycle bound to the metal centre, Pd–S(1) 2.339 9(22), Pd–S(4) 2.333 1(22), Pd–S(10) 2.326 1(22), and Pd–S(13) 2.323 9(21) Å; the two N atoms are non-bonding, Pd • • • N(7) 3.744(7) and Pd • • • N(16) 3.760(6) Å. The green complex [Pd([18]aneN$_2$S$_4$)][BPh$_4$]$_2$ crystallises in the monoclinic space group $P2_1/c$, with a = 16.888 8(12), b = 16.553 3(15), c = 18.537 6(12) Å, β = 93.144(8)°, and Z = 4. The structure of [Pd([18]aneN$_2$S$_4$)]$^{2+}$ is markedly different to that of [Pd(Me$_2$[18]aneN$_2$S$_4$)]$^{2+}$ and shows the Pd^{II} ion co-ordinated to an N$_2$S$_2$ donor set in a square-planar configuration, Pd–S(1) 2.311(3), Pd–N(7) 2.123(7), Pd–S(13) 2.357(3), and Pd–N(16) 2.068(7) Å; the S(1)–N(16)–S(13) linkage binds meridionally to the metal centre, The two remaining thioether donors interact at long range with the metal centre, Pd • • • S(10) 2.954(4) and Pd • • • S(4) 3.000(3) Å with S(4)–Pd–S(10) 158.94(9)°. The overall stereochemistry at Pd^{II} is therefore tetragonally distorted octahedral with a formal [N$_2$S$_2$ + S$_2$] co-ordination sphere. The structural differences between [Pd(Me$_2$[18]aneN$_2$S$_4$)]$^{2+}$ and [Pd([18]aneN$_2$S$_4$)]$^{2+}$ are reflected in their spectroscopic and redox properties. Cyclic voltammetry of [Pd(Me$_2$[18]aneN$_2$S$_4$)][PF$_6$]$_2$ in MeCN (0.1 mol dm^{-3} NBu$^n_4$PF$_6$ supporting electrolyte) at platinum electrodes shows a chemically reversible one-electron reduction at $E_{\frac{1}{2}}$ = −0.74 V *vs.* ferrocene–ferrocenium. Controlled potential electrolysis affords a bright yellow paramagnetic species which has been assigned on the basis of coulometry, e.s.r. and u.v.–visible spectroelectrochemistry as a mononuclear d^9 Pd^{I} species. No oxidative activity is observed for [Pd(Me$_2$[18]aneN$_2$S$_4$)][PF$_6$]$_2$ within the range of the solvent up to +2.0 V. In contrast, cyclic voltammetry of [Pd([18]aneN$_2$S$_4$)][PF$_6$]$_2$ shows a chemically reversible one-electron oxidation at $E_{\frac{1}{2}}$ = +0.57 V *vs.* ferrocene-ferrocenium (ΔE_p = 195 mV at a scan rate of 150 mV s^{-1}). Controlled potential electrolysis affords a bright-red paramagnetic product which is assigned on the basis of coulometry, e.s.r. and u.v.–visible spectroelectrochemistry as a mononuclear d^7 Pd^{III} species. Two irreversible reductions are also observed for [Pd([18]aneN$_2$S$_4$)][PF$_6$]$_2$ at E_{pc} = −1.01 and −1.54 V *vs.* ferrocene–ferrocenium. Reaction of PdCl$_2$ with Me$_2$[18]aneN$_2$S$_4$ or [18]aneN$_2$S$_4$ in a 2:1 molar ratio affords the corresponding binuclear complexes [Pd$_2$Cl$_2$(Me$_2$[18]aneN$_2$S$_4$)]$^{2+}$ and [Pd$_2$Cl$_2$([18]aneN$_2$S$_4$)]$^{2+}$. The complex [Pd$_2$Cl$_2$([18]aneN$_2$S$_4$)][PF$_6$]$_2$·2MeCN crystallises in the monoclinic space group $C2/c$, with a = 18.617(13), b = 15.569(11), c = 14.323(14) Å, β = 113.59(5)°, and Z = 4. The single crystal *X*-ray structure of [Pd$_2$Cl$_2$([18]aneN$_2$S$_4$)]$^{2+}$ shows each Pd^{II} bound in a square plane to two S-donors, Pd–S(1) 2.317(4), and Pd–S(7) 2.316(4) Å, and to one N-donor, Pd–N(4) 2.049(13) Å, of the macrocycle, and a terminal Cl$^-$ ligand, Pd–Cl 2.305(4) Å. The Cl$^-$ ligand is displaced out of the least-squares plane S(1)–N(4)–S(7)–Pd by 0.0712 Å due to the steric influence of the central methylene groups bridging the S-donors. The closest non-bonded interaction of 3.406(2) Å is between two Pd atoms in adjacent molecules related by a crystallographic two-fold axis. The intramolecular Pd • • • Pd distance is 4.196(2) Å. The synthesis and structures of the analogous mono- and bi-nuclear Pt^{II} complexes [Pt(Me$_2$[18]aneN$_2$S$_4$)]$^{2+}$, [Pt([18]aneN$_2$S$_4$)]$^{2+}$, and [Pt$_2$Cl$_2$([18]aneN$_2$S$_4$)]$^{2+}$ are also discussed.

† *Supplementary data available:* see Instructions for Authors, *J. Chem. Soc., Dalton Trans.*, 1990, Issue 1, pp. xix—xxii.

Non-S.I. unit employed: G = 10^{-4} T.

We have been investigating the synthesis and redox properties of macrocyclic complexes of the platinum group metals.[1,2] In the course of this study the effectiveness of homoleptic poly-thia and -aza macrocyclic co-ordination to stabilise Pd^{III},[3,4] Pt^{III},[5] and Pd^{I} [6,7] has been demonstrated. We wished to extend this work to the study of the co-ordination chemistry of the mixed *S*- and *N*-donor macrocycles [18]aneN_2S_4 (1,4,10,13-tetrathia-7,16-diazacyclo-octadecane) and Me_2[18]aneN_2S_4 (7,16-dimethyl-1,4,10,13-tetrathia-7,16-diazacyclo-octadecane)[8,9] with Pd^{II} and Pt^{II} centres. In particular, we were interested in

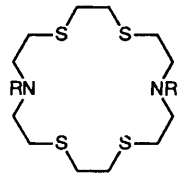

[18]aneN_2S_4; R = H

Me_2[18]aneN_2S_4; R = Me

monitoring the co-ordinative flexibility of these large-ring systems, since the stereochemical requirements of these potentially hexadentate ligands are not compatible with the four-co-ordinate, square-planar geometries preferred by Pd^{II} and Pt^{II} centres.

We report herein the synthesis and characterisation of mono- and bi-nuclear Pd^{II} and Pt^{II} complexes incorporating [18]aneN_2S_4 and Me_2[18]aneN_2S_4. A full spectroelectrochemical study of the two mononuclear palladium species is also presented. A preliminary communication on this work has appeared.[10]

Results and Discussion

Palladium.—Treatment of $PdCl_2$ with 1 molar equivalent of Me_2[18]aneN_2S_4 in refluxing MeCN–H_2O affords an orange solution. Addition of an excess of NH_4PF_6 gives an orange product which can be recrystallised from MeCN. The fast-atom bombardment (f.a.b.) mass spectrum of the complex exhibits molecular ion peaks at *m/z* 604 and 460 corresponding to $[^{106}Pd(Me_2[18]aneN_2S_4 - H)PF_6]^+$ and $[^{106}Pd(Me_2[18]aneN_2S_4)]^+$ respectively. These data, together with elemental analyses and i.r. spectroscopy, confirm the formulation $[Pd(Me_2[18]aneN_2S_4)][PF_6]_2$. The ^1H n.m.r. spectrum of the complex in CD_3CN shows a singlet resonance at δ 2.48 due to the methyl protons. A complex second-order multiplet in the range δ 2.68—3.50 is assigned to the methylene protons of the ring. Carbon-13 DEPT n.m.r. spectroscopy of $[Pd(Me_2[18]aneN_2S_4)]^{2+}$ in CD_3CN shows four distinct resonances at δ 49.87, 40.31, 39.40 (CH_2), and 41.57 p.p.m. (CH_3). These data confirm the presence of only one isomer in solution, and are consistent with a square-planar stereochemistry around the Pd^{II} centre.

The single-crystal *X*-ray structure of $[Pd(Me_2[18]aneN_2S_4)][PF_6]_2 \cdot Me_2CO$ is in agreement with solution studies: the structure determination shows square-planar co-ordination of the four thioether donors of the macrocycle to the Pd^{II} ion, Pd–S(1) 2.339 9(22), Pd–S(4) 2.333 1(22), Pd–S(10) 2.326 1(22), and Pd–S(13) 2.323 9(21) Å [Figure 1(*a*)]. The two NMe functions are orientated away from, and do not interact with, the metal centre, Pd • • • N(7) 3.744(7) and Pd • • • N(16) 3.760(6) Å [Figure 1(*b*)]. The macrocycle, therefore, co-ordinates to the Pd^{II} centre as a simple tetradentate thioether donor.

The corresponding reaction of $PdCl_2$ with the non-

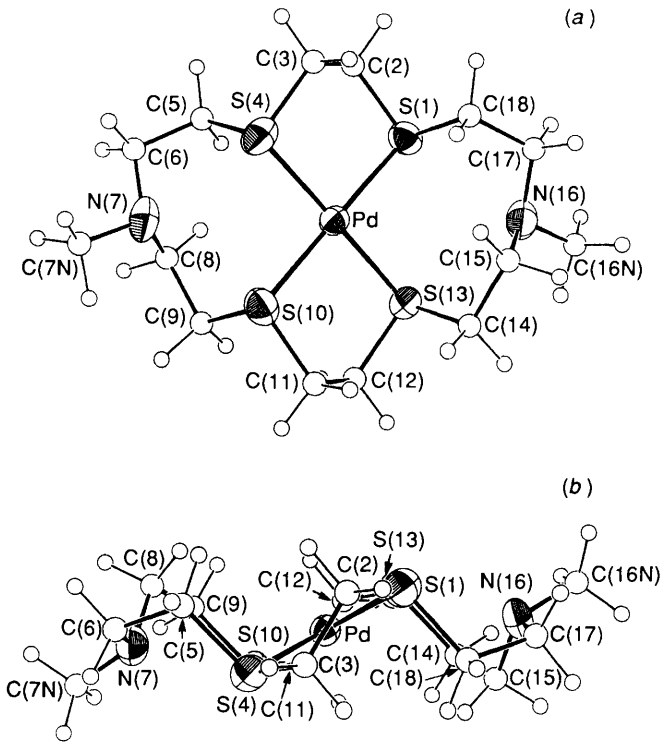

Figure 1. *X*-Ray crystal structure of $[Pd(Me_2[18]aneN_2S_4)]^{2+}$: (*a*) top view, (*b*) side view with numbering scheme adopted

methylated crown [18]aneN_2S_4, however, affords a different type of product. Treatment of $PdCl_2$ with 1 molar equivalent of [18]aneN_2S_4 in refluxing MeCN in the presence of 2.2 molar equivalents of $TlPF_6$ gives a purple solution with a white precipitate of TlCl. Removal of TlCl by filtration and of the solvent *in vacuo* yields a blue residue which can be recrystallised from H_2O to afford a dark blue product. The f.a.b. mass spectrum of this product shows peaks with the correct isotopic distribution at *m/z* and 431 assigned to $[^{106}Pd([18]aneN_2S_4)PF_6]^+$ and $[^{106}Pd([18]aneN_2S_4 - H)]^+$ respectively. On the basis of these data, together with elemental analyses and i.r. spectroscopy, the product can be assigned as $[Pd([18]aneN_2S_4)][PF_6]_2$. The ^{13}C DEPT n.m.r. spectrum of $[Pd([18]aneN_2S_4)]^{2+}$ measured in $(CD_3)_2CO$ at 298 K, exhibits six broad, ill-resolved resonances at δ 56.28, 51.12, 47.26, 34.05, 31.88, and 27.29 p.p.m. suggesting possible fluxional behaviour in solution. Cooling to 208 K does not, however, lead to significant sharpening of the spectrum. The ^1H n.m.r. spectrum of the complex in $(CD_3)_2CO$ at 298 K shows a broad second-order multiplet at δ 3.70—2.56, assigned to the macrocyclic methylene protons, and a resonance at δ 5.00 assigned to the NH protons on the basis of its disappearance on addition of D_2O. Cooling this sample to 223 K leads to a sharpening of the methylene proton signals. The complex $[Pd([18]aneN_2S_4)][PF_6]_2$ dissolves in MeCN to give a purple solution, the electronic spectrum of which shows bands at $\lambda_{max.}$ = 514 (ε = 124), 322 (2 815), 266 (9 420), and 233 nm (12 140 $dm^3\ mol^{-1}\ cm^{-1}$). The last band is assigned tentatively to a S→M charge-transfer transition.

It was clear from the spectroscopic data that the co-ordination geometry at Pd^{II} in $[Pd([18]aneN_2S_4)]^{2+}$ was not simply square planar as in the case of $[Pd(Me_2[18]aneN_2S_4)]^{2+}$. In order to elucidate the stereochemistry and co-ordination sphere around the Pd^{II} centre in $[Pd([18]aneN_2S_4)]^{2+}$, a single-crystal *X*-ray structure determination was undertaken. Green columnar crystals were obtained by metathesis of the PF_6^- salt with $NaBPh_4$ in H_2O, followed by

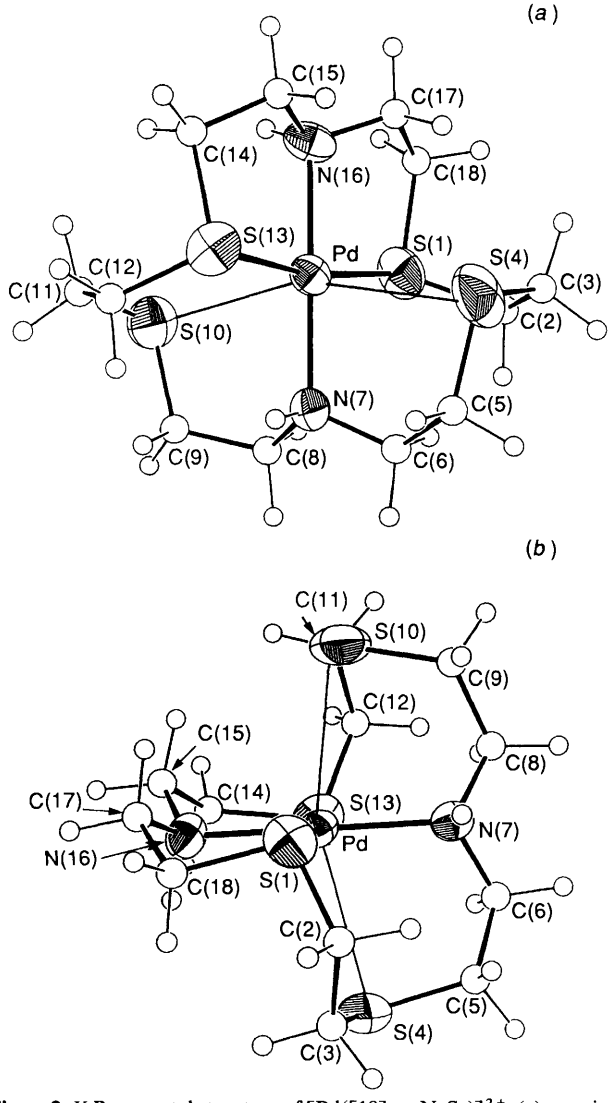

Figure 2. *X*-Ray crystal structure of $[Pd([18]aneN_2S_4)]^{2+}$: (*a*) top view, (*b*) side view with numbering scheme adopted

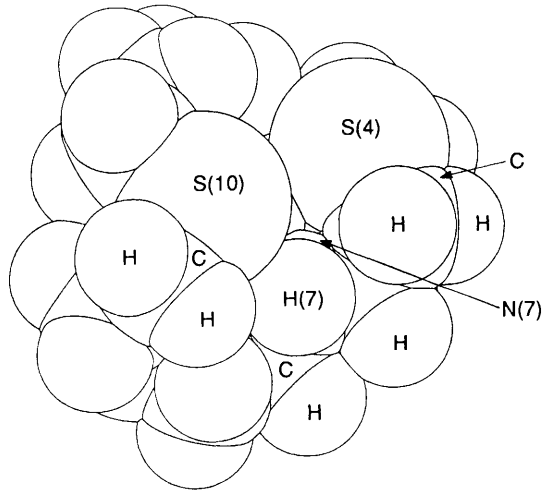

Figure 3. Space-filling diagram of $[Pd([18]aneN_2S_4)]^{2+}$

recrystallisation from $MeNO_2$. The structure of $[Pd([18]aneN_2S_4)]^{2+}$ (Figure 2) shows the Pd^{II} ion co-ordinated to an N_2S_2 donor set in a square-planar configuration, Pd–S(1) 2.311(3), Pd–N(7) 2.123(7), Pd–S(13) 2.357(3), and Pd–N(16) 2.068(7) Å, with the S(1)–N(16)–S(13) linkage binding meridionally to the metal centre. The two remaining thioether donors interact at long range with the metal centre, Pd • • • S(10) 2.954(4) and Pd • • • S(4) 3.000(3) Å, and lie respectively 2.863 Å above and 2.901 Å below the Pd–S(1)–N(7)–S(13)–N(16) least-squares plane, S(4) • • • Pd • • • S(10) 158.94(9)°. The co-ordination at Pd^{II} is therefore tetragonally distorted octahedral with a formal $[N_2S_2 + S_2]$ co-ordination sphere. The approach of the two thioether donors at long range is probably responsible for the elongation [0.055(10) Å] of the Pd–N(7) bond relative to Pd–N(16). Interestingly, the hexathia analogue $[Pd([18]aneS_6)]^{2+}$ ($[18]aneS_6$ = 1,4,7,10,13,16-hexathiacyclo-octadecane) exhibits a different geometry with the macrocycle adopting an S-shaped double boat conformation involving long-range, weak interaction of the two apical *S*-donors, Pd • • • S_{ap} 3.273 0(17) Å, to a square-planar PdS_4 moiety, Pd–S_{eq} 2.311 4(14) and 2.306 7(15) Å.[11] The long-range interactions between Pd^{II} and the apical sulphur donors observed in the solid-state structure of $[Pd([18]aneN_2S_4)]^{2+}$ suggest modes of co-ordinative flexibility which may account for the apparent fluxionality of the species in solution.

A comparison of the crystal structures of $[Pd([18]aneN_2S_4)]^{2+}$ and $[Pd(Me_2[18]aneN_2S_4)]^{2+}$ demonstrates that replacement of the NH functions by NMe has a remarkable influence on the stereochemistry around Pd^{II}. A space-filling diagram of $[Pd([18]aneN_2S_4)]^{2+}$ (Figure 3) suggests that this difference may be attributable to the steric effect of the NMe groups. In $[Pd([18]aneN_2S_4)]^{2+}$, the Pd^{II} ion is fully encapsulated by the $[N_2S_2 + S_2]$ co-ordination of the crown and the N sites are sterically crowded within the macrocyclic fold. Replacement of the NH functions by NMe groups would, therefore, force a conformational and stereochemical change since there is insufficient space to accommodate the *N*-donor methyl groups in the observed solid-state structure of $[Pd([18]aneN_2S_4)]^{2+}$.

Platinum.—The complex $[Pt(Me_2[18]aneN_2S_4)][PF_6]_2$ can be prepared by an analogous method to $[Pd(Me_2[18]aneN_2S_4)][PF_6]_2$. The f.a.b. mass spectrum of the resulting cream solid exhibits molecular ion peaks at *m/z* 694 and 549 assigned to $[^{195}Pt(Me_2[18]aneN_2S_4)PF_6]^+$ and $[^{195}Pt(Me_2[18]aneN_2S_4)]^+$ respectively. The ^1H n.m.r. spectrum of $[Pt(Me_2[18]aneN_2S_4)]^{2+}$ shows a singlet resonance at δ 2.46 corresponding to the methyl protons, and second-order patterns at δ 3.18—3.30 and 3.55—3.62 corresponding to 16 protons of the methylene groups adjacent to the *S*-donor atoms. Multiplets at δ 2.54—2.62 and 2.80—2.87 are assigned to the eight methylene groups adjacent to the *N*-donors. The ^{13}C DEPT n.m.r. spectrum of $[Pt(Me_2[18]aneN_2S_4)]^{2+}$ is almost identical to that of the Pd^{II} analogue with one methyl carbon resonance at δ 40.83 p.p.m. and three distinct methylene carbon resonances at δ 49.18, 39.87, and 39.28 p.p.m. This suggests that $[Pt(Me_2[18]aneN_2S_4)]^{2+}$ and $[Pd(Me_2[18]aneN_2S_4)]^{2+}$ are isostructural.

The yellow Pt^{II} complex, $[Pt([18]aneN_2S_4)][PF_6]_2$, can also be prepared. The f.a.b. mass spectrum of this complex shows peaks with the correct isotopic distribution at *m/z* 667 and 521 assigned to $[^{195}Pt([18]aneN_2S_4 + H)PF_6]^+$ and $[^{195}Pt([18]aneN_2S_4)]^+$ respectively. The ^1H n.m.r. spectrum of $[Pt([18]aneN_2S_4)]^{2+}$ in CD_3CN at 298 K shows an NH resonance at δ 5.68 as well as a broad, second-order multiplet due to the macrocyclic methylene protons in the range δ 3.42—2.84 p.p.m. The ^{13}C DEPT n.m.r. spectrum measured at 298 K, 50.32 MHz, shows five broadened methylene carbon resonances at δ 55.39, 53.11, 36.84, 34.74, and 28.08 p.p.m. Re-running the spectrum at 90.56 MHz in $(CD_3)_2CO$ reveals methylene carbon resonances at δ 56.1 (NCH_2, 2 C), 53.8 (NCH_2, 2 C), 46.6, 42.0,

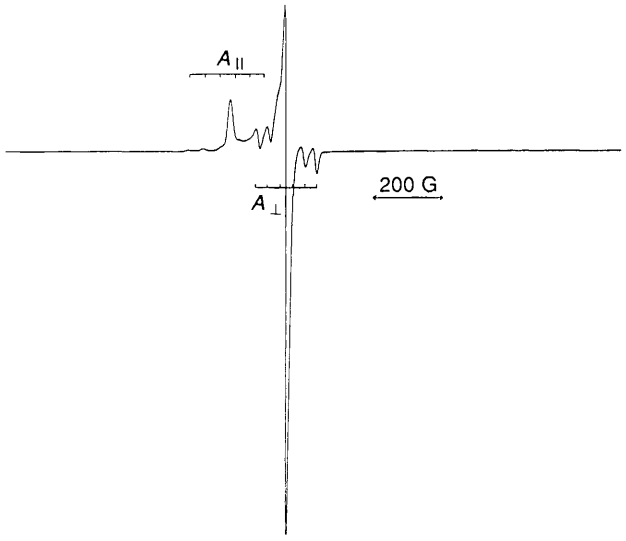

Figure 4. *X*-Band e.s.r. spectrum (77 K, MeCN, 0.1 mol dm^{-3} $NBu^n_4PF_6$) of d^9 $[Pd(Me_2[18]aneN_2S_4)]^+$ generated electrochemically

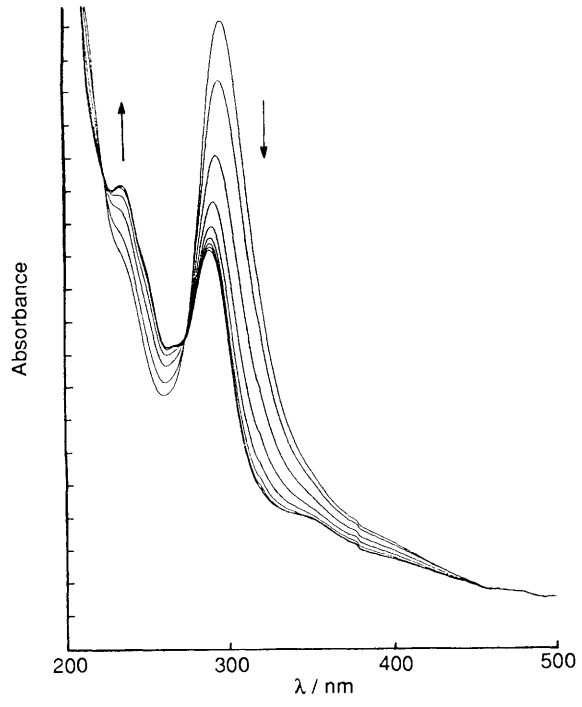

Figure 5. Reduction of $[Pd(Me_2[18]aneN_2S_4)]^{2+}$ to $[Pd(Me_2[18]aneN_2S_4)]^+$ measured in MeCN (0.1 mol dm^{-3} $NBu^n_4PF_6$) at 248 K

38.3, 37.3, 35.3 (2 C), 28.2, and 26.3 p.p.m. (SCH_2, total of 8 C). On the basis of these spectroscopic data and in the absence of crystallographic analysis, we cannot confidently assign a stereochemistry to $[Pt([18]aneN_2S_4)]^{2+}$; indeed more than one isomer may be present in solution. An elongated square-based pyramidal geometry with $[S_4 + S]$ co-ordination has been observed for $[Pt([9]aneS_3)_2]^{2+}$ ([9]$aneS_3$ = 1,4,7-trithiacyclononane), Pt–S_{eq} 2.25—2.30 and Pt · · · S_{ap} 2.88 Å, with the sixth thioether donor atom non-co-ordinating, Pt · · · S 4.04 Å;[5] a related square-based pyramidal structure may be occurring for $[Pt([18]aneN_2S_4)]^{2+}$. Interestingly, the Pd^{II} complex $[Pd([9]aneS_3)_2]^{2+}$ shows $[S_4 + S_2]$ co-ordination and is therefore not isostructural with the Pt^{II} analogue $[Pt([9]aneS_3)_2]^{2+}$; the Pd^{II} and Pt^{II} complexes of $[18]aneN_2S_4$ may have differing structures both in the solid state and in solution.

Electrochemical Study of $[ML]^{2+}$ (M = Pd *or* Pt, L = $[18]aneN_2S_4$ *or* $Me_2[18]aneN_2S_4$).—In view of the paucity of genuine monomeric d^7 or d^9 Pt and Pd complexes, and the recently reported successful stabilisation of these +1 and +3 metal oxidation states by polythia and polyaza macrocyclic ligands,[1-5] an investigation of the redox and electronic properties of $[M([18]aneN_2S_4)]^{2+}$ and $[M(Me_2[18]aneN_2S_4)]^{2+}$ (M = Pd or Pt) was initiated.

$[M(Me_2[18]aneN_2S_4)]^{2+}$ (M = Pd *or* Pt). Cyclic voltammetry of $[Pd(Me_2[18]aneN_2S_4)][PF_6]_2$ in MeCN (0.1 mol dm^{-3} $NBu^n_4PF_6$) reveals a chemically reversible reduction occurring at $E_{\frac{1}{2}} = -0.74$ V *vs.* ferrocene–ferrocenium (ΔE_p = 72 mV at a scan rate of 100 mV s^{-1}). Coulometry confirms that this reduction corresponds to a one-electron process (n = 1.08). The e.s.r. spectrum of the bright yellow reduction product, measured at 77 K as a frozen glass in MeCN, shows (Figure 4) a strong anisotropic signal with axial symmetry, $g_{\parallel} = 2.155$ and $g_{\perp} = 2.049$. In the $g_{\perp}$ region, the first, second, fifth, and sixth features of the hyperfine coupling to ^{105}Pd ($I = \frac{5}{2}$, 22.2%) are evident, giving $A_{\perp} = 34$ G. Similarly, close examination of the $g_{\parallel}$ region allows the first and second features to be discerned, giving $A_{\parallel} = 48$ G. These data are consistent with the formation of a metal-based d^9 Pd^I radical.[6,7,12] Interestingly, the g values for this species are closer to free-spin (2.0023) than those for the only other macrocyclic Pd^I monomers reported, namely $[Pd(Me_4[14]aneN_4)]^+$ ($Me_4[14]aneN_4$ = 1,4,8,11-tetramethyl-1,4,8,11-tetraazacyclotetradecane) ($g_{\parallel} = 2.302$, $g_{\perp}$ = 2.076)[6] and $[Pd(Bz_4[14]aneN_4)]^+$(Bz[14]$aneN_4$ = 1,4,8,11-tetrabenzyl-1,4,8,11-tetraazacyclotetradecane) ($g_{\parallel} = 2.320$, $g_{\perp} = 2.086$),[7] indicating a greater degree of covalency in $[Pd(Me_2[18]aneN_2S_4)]^+$. This can be attributed to the relative π-acidity of the thioether donors, which allows some delocalisation of electron density onto the S-donors. The reduction of $[Pd(Me_2[18]aneN_2S_4)]^{2+}$ to $[Pd(Me_2[18]aneN_2S_4)]^+$ was studied spectroelectrochemically using an optically transparent electrode system. Importantly, the spectral changes on reduction of $[Pd(Me_2[18]aneN_2S_4)]^{2+}$ (Figure 5) show the process to occur both reversibly and isosbestically (λ_{iso} = 224 and 274 nm); for $[Pd(Me_2[18]aneN_2S_4)]^{2+}$: $\lambda_{max.}$ = 373 ($\varepsilon_{max.}$ = 3 000), 298 (14 460), and 232 nm (15 070 dm^3 mol^{-1} cm^{-1}); for $[Pd(Me_2[18]aneN_2S_4)]^+$: $\lambda_{max.}$ = 290 ($\varepsilon_{max.}$ = 9 300) and 235 nm (10 440 dm^3 mol^{-1} cm^{-1}) thus precluding the formation of any long-lived intermediates during the one-electron reduction. The loss of intensity and the shift to higher energy (to 290 nm) of the band at 298 nm (assigned to a S→M charge-transfer transition) on reduction of the 2+ cation is consistent with increased electron density at the metal centre. The complex $[Pd(Me_2[18]aneN_2S_4)]^{2+}$ can be regenerated quantitatively by oxidation of $[Pd(Me_2[18]aneN_2S_4)]^+$.

Cyclic voltammetry of $[Pd(Me_2[18]aneN_2S_4)]^{2+}$ also shows an irreversible reduction at $E_{pc} = -1.83$ V *vs.* ferrocene–ferrocenium assigned tentatively to a Pd^I–Pd^0 couple; no oxidative activity is observed for the complex within the range of the solvent up to +2.0 V.

The cyclic voltammogram of $[Pt(Me_2[18]aneN_2S_4)][PF_6]_2$, measured under the same conditions as above, shows an irreversible reduction at $E_{pc} = -1.52$ V *vs.* ferrocene–ferrocenium; we would expect a mononuclear Pt^I species to be quenched rapidly, most probably via disproportionation, or via dimerisation involving metal–metal bond formation. No examples of genuine monomeric d^9 Pt^I co-ordination complexes have been reported in the literature. A second irreversible reduction is also observed at $E_{pc} = -2.08$ V *vs.* ferrocene–ferrocenium; like $[Pd(Me_2[18]aneN_2S_4)]^{2+}$, $[Pt(Me_2[18]aneN_2S_4)]^{2+}$ shows no oxidative process within the range of the solvent.

$[M([18]aneN_2S_4)]^{2+}$ (M = Pd *or* Pt). Cyclic voltammetry

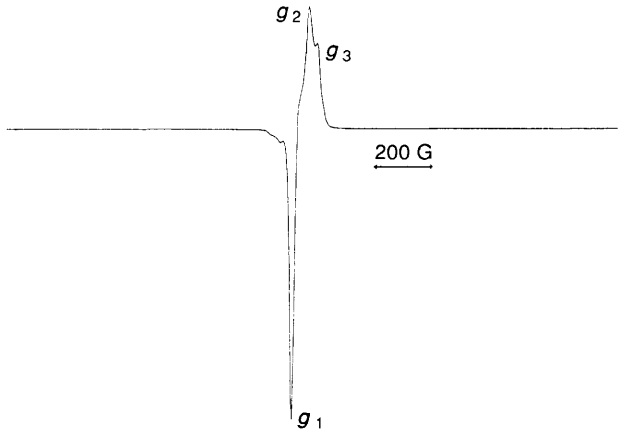

Figure 6. *X*-Band e.s.r. spectrum (77 K, MeCN, 0.1 mol dm^{-3} $NBu^n_4PF_6$) of d^7 $[Pd([18]aneN_2S_4)]^{3+}$ generated electrochemically

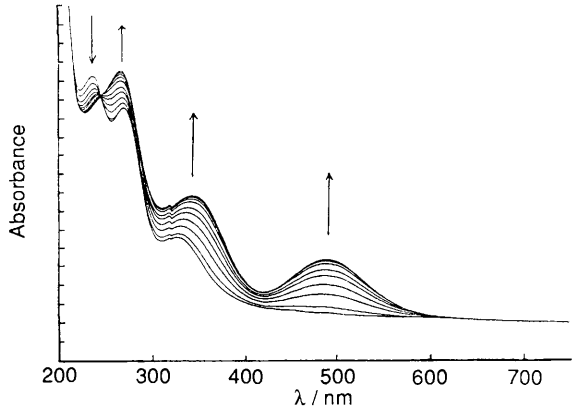

Figure 7. Oxidation of $[Pd([18]aneN_2S_4)]^{2+}$ to $[Pd([18]aneN_2S_4)]^{3+}$ measured in MeCN (0.1 mol dm^{-3} $NBu^n_4PF_6$) at 298 K

of $[Pd([18]aneN_2S_4)][PF_6]_2$ in MeCN (0.1 mol dm^{-3} $NBu^n_4PF_6$ supporting electrolyte) at platinum electrodes shows a chemically reversible oxidation at $E_{\frac{1}{2}} = +0.57$ V *vs.* ferrocene–ferrocenium ($\Delta E_p = 195$ mV at a scan rate of 150 mV s^{-1}). Coulometry confirms that this oxidation corresponds to a one-electron process ($n = 0.95$). The e.s.r. spectrum of the bright-red oxidation product, measured at 77 K as a frozen glass in MeCN, shows (Figure 6) a strong rhombic signal with $g_1 = 2.064$, $g_2 = 2.052$, and $g_3 = 2.019$. These spectral features are consistent with the formation of the d^7 Pd^{III} species, $[Pd([18]aneN_2S_4)]^{3+}$.[3,4,13] Unresolved hyperfine coupling to ^{105}Pd ($I = \frac{5}{2}$, 22.2%) is observed in the low-field portion of the spectrum. Comparable spectral features have been observed for $[Pd([9]aneS_3)_2]^{3+}$[3] and $[Pd([9]aneN_3)_2]^{3+}$ ([9]aneN$_3$ = 1,4,7-triazacyclononane).[4] The oxidation of Pd^{II} to Pd^{III} was also monitored spectroelectrochemically using an optically transparent electrode system. Conversion of $[Pd([18]aneN_2S_4)]^{2+}$ to $[Pd([18]aneN_2S_4)]^{3+}$ occurs reversibly and isosbestically ($\lambda_{iso} = 241$ nm) (Figure 7); for $[Pd([18]aneN_2S_4)]^{2+}$: $\lambda_{max.} = 514$ ($\varepsilon = 124$), 332 (2 815), 266 (9 420), and 233 nm (12 140 dm^3 mol^{-1} cm^{-1}); for $[Pd([18]aneN_2S_4)]^{3+}$: $\lambda_{max.} = 488$ ($\varepsilon_{max.} = 3\,180$), 341 (5 890), and 264 nm (11 170 dm^3 mol^{-1} cm^{-1}).

Cyclic voltammetry of $[Pd([18]aneN_2S_4)][PF_6]_2$ also shows a quasi-reversible oxidation at $E_{pa} = +1.30$ V *vs.* ferrocene–ferrocenium assigned to a Pd^{III}–Pd^{IV} couple; two irreversible reductions are observed at $E_{pc} = -1.01$ and -1.54 V *vs.* ferrocene–ferrocenium.

A preliminary electrochemical study of $[Pt([18]aneN_2S_4)][PF_6]_2$ was undertaken. The cyclic voltammogram of $[Pt([18]aneN_2S_4)]^{2+}$ shows an extremely broad oxidation wave centred at $E_{pa} = +1.07$ V with a broad return wave at $E_{pc} = -0.01$ V *vs.* ferrocene–ferrocenium. These have an unusually large peak separation, $\Delta E_p = 1\,080$ mV at a scan rate of 330 mV s^{-1}. Coulometric measurements suggest the oxidation to be a two-electron process with the solution changing initially from pale yellow to bright yellow and finally to golden yellow. A sample of the bright yellow solution shows a weak rhombic e.s.r. signal (77 K, MeCN glass) with $g_1 = 2.115$, $g_2 = 2.049$, and $g_3 = 1.987$, consistent with the formation of a transient mononuclear Pt^{III} species. Hyperfine coupling to ^{195}Pt ($I = \frac{1}{2}$, 33.7%) is difficult to discern due to the weakness of the signal. The final golden solution is diamagnetic. These results suggest that the oxidation process involves overlapping II–III and III–IV redox couples. Clearly the broad oxidation wave for $[Pt([18]aneN_2S_4)]^{2+}$ suggests that a major stereochemical change occurs at the metal centre upon oxidation. Significantly, the value of $E_{pa} = +1.07$ V for the oxidation of $[Pt([18]aneN_2S_4)]^{2+}$ is more anodic than for the Pd^{II} analogue. This is opposite to the expected trend for the oxidation of Pd^{II} and Pt^{II} complexes and suggests that the 2+ cations are not isostructural. The structure of $[Pd([18]aneN_2S_4)]^{2+}$ shows a quasi-six-co-ordinate [N_2S_2 + S_2] co-ordination in the solid state; for the oxidation of the Pt^{II} analogue to occur at a more anodic potential, its stereochemistry must involve greater interaction between the Pt^{II} centre and the thioether donors. On the basis of the n.m.r. data above, square-planar S_4 co-ordination appears unlikely and this leads us to prefer a five-co-ordinate stereochemistry for $[Pt([18]aneN_2S_4)]^{2+}$. The complex $[Pt([18]aneN_2S_4)]^{2+}$ also shows an irreversible reduction at $E_{pc} = -1.77$ V *vs.* ferrocene–ferrocenium.

Binuclear Complexes of $[18]aneN_2S_4$.—In view of the co-ordinative versatility of $[18]aneN_2S_4$ and $Me_2[18]aneN_2S_4$ in mononuclear Pd and Pt complexes, an investigation of the ability of these macrocyclic ligands to function as binucleating agents was initiated.

Reaction of 2 molar equivalents of $PdCl_2$ with 1 molar equivalent of $[18]aneN_2S_4$ in refluxing MeCN–H_2O yielded a golden yellow solution. Addition of PF_6^- counter-ion and recrystallisation from MeCN gave the product as yellow needles. The i.r. spectrum of the complex exhibited peaks characteristic of a co-ordinated macrocycle and PF_6^- counter-ion. Additionally, the single absorption apparent at 330 cm^{-1} is indicative of a terminal Pd–Cl stretching vibration, ν(Pd–Cl). F.a.b. mass spectrometry of the complex reveals molecular ion peaks at *m/z* 609, 575, 539, and 431 which are assigned to $[^{106}Pd_2{}^{35}Cl_2([18]aneN_2S_4 + H)]^+$, $[^{106}Pd_2{}^{35}Cl([18]aneN_2S_4 + 2H)]^+$, $[^{106}Pd_2([18]aneN_2S_4 + H)]^+$, and $[^{106}Pd([18]aneN_2S_4 - H)]^+$ respectively. The ^1H n.m.r. spectrum of the product shows complex second-order multiplets in the ranges δ 2.7—3.6 and 4.2—4.6 due to the macrocyclic methylene protons, while the ^{13}C DEPT n.m.r. spectrum shows three distinct methylene carbon resonances at δ 54.77 (NCH_2, 4 C), 38.28 (NCH_2CH_2S, 4 C), and 30.44 p.p.m. (SCH_2CH_2S, 4 C). This evidence, combined with elemental analytical data, confirms the assignment of the product as $[Pd_2Cl_2([18]aneN_2S_4)][PF_6]_2$. The analogous binuclear Pt^{II} complex, $[Pt_2Cl_2([18]aneN_2S_4)][PF_6]_2$, was prepared by a similar method, and characterised by i.r. [ν(Pt–Cl) = 330 cm^{-1}], ^1H n.m.r., and f.a.b. mass spectroscopy and elemental analysis.

A single-crystal *X*-ray structure determination of $[Pd_2Cl_2([18]aneN_2S_4)][PF_6]_2 \cdot 2MeCN$ was undertaken to confirm the nature of the donor set to each Pd^{II} centre, and to reveal the conformation of the co-ordinated macrocycle. The structure shows (Figure 8) the cation sitting across a crystallographic inversion centre, with a two-fold rotation axis (C_2) relating adjacent molecules within the crystal lattice. Each Pd^{II} centre is

bound by a square plane consisting of two S-donors and one N-donor of the macrocycle and a terminal Cl^- ligand, Pd–S(1) 2.317(4), Pd–S(7) 2.316(4), Pd–N(4) 2.049(13), and Pd–Cl 2.305(4) Å. The Cl^- ligands are displaced out of the S(1)–N(4)–S(7)–Pd least-squares plane by 0.0712 Å due to the steric influence of the central methylene groups bridging the S-donors. Interestingly, the closest non-bonded Pd · · · Pd interaction of 3.406(2) Å occurs between adjacent molecules related by the crystallographic two-fold axis (Figure 9). The intramolecular Pd · · · Pd distance is 4.196(2) Å indicating that the two metals are non-interacting. Lehn and co-workers[14] have reported a similar NS_2Cl donor set for each Pd^{II} centre in binuclear complexes derived from 2,6-functionalised pyridyl ligands.

Conclusion

The results from this study show that $[Pd([18]aneN_2S_4)]^{2+}$ and its di-*N*-methylated analogue $[Pd(Me_2[18]aneN_2S_4)]^{2+}$ adopt completely different stereochemistries, the former preferring a formal $[N_2S_2 + S_2]$ donor set in a distorted octahedral geometry, while for the latter, an S_4 co-ordination in a square plane is observed. These stereochemical differences are reflected in the electrochemical properties of the complexes, with the non-methylated system stabilising mononuclear Pd^{III}, while the methylated system is particularly effective for the stabilisation of mononuclear Pd^{I}. These are highly unusual monomers, the normal oxidation states for Pd being 0, II, and IV. In addition, most Pd^{I} and Pd^{III} complexes reported previously are diamagnetic dimers involving direct Pd–Pd bonds.[15] Relatively simple macrocyclic ligands can, therefore, stabilise otherwise unobtainable metal radical species *selectively*.

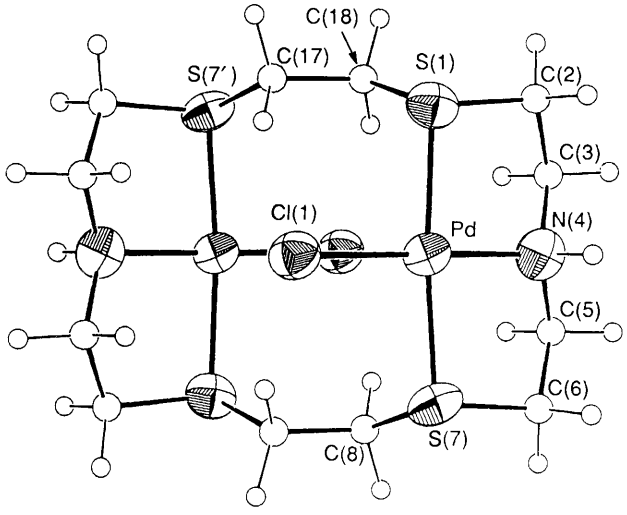

Figure 8. Top view of the *X*-ray crystal structure of $[Pd_2Cl_2([18]aneN_2S_4)]^{2+}$ with numbering scheme adopted. Primed atoms are related to their unprimed equivalents by inversion through $(0, 0, \frac{1}{2})$

The generation of $[Pd([18]aneN_2S_4)]^{3+}$ from the [4 + 2] co-ordinate $[Pd([18]aneN_2S_4)]^{2+}$ depends on the availability of distorted octahedral stereochemistries for both species. Indeed, the large peak-to-peak separation in the cyclic voltammogram (ΔE_p = 195 mV at a scan rate of 150 mV s^{-1}) is indicative of a major stereochemical change occurring at the metal upon oxidation. Presumably the long-range apical S-donors move towards the metal centre on oxidation to neutralise the extra positive charge at the metal centre, and to set up the Jahn–Teller distorted octahedral co-ordination sphere preferred by the d^7 metal ions. Interestingly, cyclic voltammetry of the related hexathia system $[Pd([18]aneS_6)]^{2+}$ under the same conditions reveals no oxidative process in the range 0 to +2.0 V. However, chemical oxidation of $[Pd([18]aneS_6)]^{2+}$ does occur slowly to generate the red $[Pd([18]aneS_6)]^{3+}$ cation which has been characterised structurally and shows[16] a Jahn–Teller elongated octahedral co-ordination very similar to that observed in $[Pd([9]aneS_3)_2]^{3+}$.[3] This shows clearly that ligand conformation is a crucial factor in metal-based oxidation processes, and suggests that there may be significant conformational and kinetic barriers to the formation of the Pd^{III} complex of $[18]aneS_6$ and the Pt^{III} complex of $[18]aneN_2S_4$. The Pd^{II}–Pd^{III} couple in $[Pd([18]aneN_2S_4)]^{2+}$ is intermediate between those observed for $[Pd([9]aneN_3)_2]^{2+/3+}$[4] and $[Pd([9]aneS_3)_2]^{2+/3+}$,[3] consistent with the presence of two hard N-donors and four softer S-donors.

Recently, Sauvage and co-workers[17] have shown that d^9 Ni^{I} centres can be stabilised *via* tetrahedral co-ordination by interlocking catenand ligands. It seems possible that stabilisation of d^9 Pd^{I} by $Me_2[18]aneN_2S_4$ might involve a similar tetrahedral distortion. This system represents the first thioether complex which exhibits a reversible Pd^{II}–Pd^{I} couple at 298 K. The reduction potential for $[Pd(Me_2[18]aneN_2S_4)]^{2+/+}$ occurs at a considerably more anodic value compared to the tetra-aza complexes, $[PdL]^{2+}$ {L = [14]aneN$_4$, $E_{\frac{1}{2}}$ = −2.10 V (quasi-reversible); $Me_4[14]aneN_4$, $E_{\frac{1}{2}}$ = −1.53 V; $Bz_4[14]aneN_4$, $E_{\frac{1}{2}}$ = −1.27 V *vs.* ferrocene–ferrocenium}.[6,7] This is attributed to the greater π-acidity of the thioether donors, and to the greater flexibility of the macrocycle, which enables the large Pd^{I} centre to be accommodated more readily.

Experimental

Infrared spectra were measured as KBr and CsI discs using a Perkin-Elmer 598 spectrometer over the range 200—4 000 cm^{-1}. U.v.–visible spectra were measured in quartz cells using Perkin-Elmer Lambda 9 and Philips Scientific SP8-400 spectrophotometers. Microanalyses were performed by the Edinburgh University Chemistry Department microanalytical service. Electrochemical measurements were performed on a Bruker E310 Universal Modular Polarograph. All readings were taken using a three-electrode potentiostatic system in MeCN containing 0.1 mol dm^{-3} $NBu^n_4PF_6$ or $NBu^n_4BF_4$ as supporting electrolyte. Cyclic voltammetric measurements were

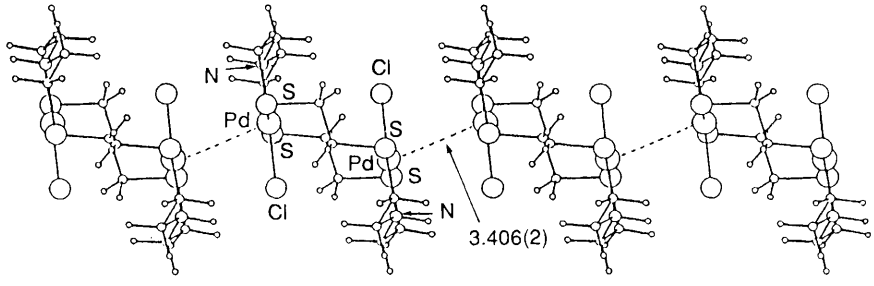

Figure 9. Packing diagram for $[Pd_2Cl_2([18]aneN_2S_4)]^{2+}$ showing intermolecular Pd · · · Pd interactions

Table 1. Bond lengths (Å), angles and torsion angles (°) with estimated standard deviations (e.s.d.s) for $[Pd(Me_2[18]aneN_2S_4)]^{2+}$

Pd–S(1)	2.339 9(22)	S(4)–C(5)	1.842(9)	N(16)–C(15)	1.450(12)	C(5)–C(6′)	1.557(20)
Pd–S(13)	2.323 9(21)	S(10)–C(9)	1.840(9)	N(16)–C(15′)	1.47(3)	C(8)–C(9)	1.547(14)
Pd–S(4)	2.333 1(22)	S(10)–C(11)	1.815(10)	N(16)–C(17)	1.467(11)	C(8′)–C(9)	1.537(20)
Pd–S(10)	2.326 1(22)	N(7)–C(6)	1.469(14)	N(16)–C(17′)	1.47(3)	C(11)–C(12)	1.488(13)
S(1)–C(2)	1.810(10)	N(7)–C(6′)	1.468(19)	N(16)–C(16N)	1.462(14)	C(14)–C(15)	1.535(13)
S(1)–C(18)	1.816(8)	N(7)–C(8)	1.455(13)	N(16)–C(16′)	1.47(4)	C(14)–C(15′)	1.53(3)
S(13)–C(12)	1.818(9)	N(7)–C(8′)	1.482(19)	C(2)–C(3)	1.515(13)	C(17)–C(18)	1.521(12)
S(13)–C(14)	1.827(9)	N(7)–C(7N)	1.469(18)	C(5)–C(6)	1.533(15)	C(17′)–C(18)	1.55(3)
S(4)–C(3)	1.809(9)	N(7)–C(7N′)	1.467(24)				

S(1)–Pd–S(13)	90.59(7)	Pd–S(4)–C(3)	101.2(3)	C(15)–N(16)–C(17)	112.7(7)	N(7)–C(8)–C(9)	108.8(8)
S(1)–Pd–S(4)	89.21(8)	Pd–S(4)–C(5)	107.6(3)	C(15)–N(16)–C(16N)	115.2(7)	N(7)–C(8′)–C(9)	108.0(12)
S(1)–Pd–S(10)	179.43(8)	C(3)–S(4)–C(5)	99.9(4)	C(15′)–N(16)–C(17′)	115.5(16)	S(10)–C(9)–C(8)	110.9(6)
S(13)–Pd–S(4)	179.52(8)	Pd–S(10)–C(9)	107.8(3)	C(15′)–N(16)–C(16′)	101.4(19)	S(10)–C(11)–C(12)	112.1(7)
S(13)–Pd–S(10)	89.00(8)	Pd–S(10)–C(11)	102.2(3)	C(17)–N(16)–C(16N)	109.2(7)	S(13)–C(12)–C(11)	112.3(6)
S(4)–Pd–S(10)	91.21(8)	C(9)–S(10)–C(11)	98.3(4)	C(17′)–N(16)–C(16′)	118.8(19)	S(13)–C(14)–C(15)	109.4(6)
Pd–S(1)–C(2)	101.1(3)	C(6)–N(7)–C(8)	111.3(8)	S(1)–C(2)–C(3)	111.6(7)	N(16)–C(15)–C(14)	110.1(8)
Pd–S(1)–C(18)	109.7(3)	C(6)–N(7)–C(7N)	107.0(9)	S(4)–C(3)–C(2)	111.0(6)	N(16)–C(15′)–C(14)	108.8(17)
C(2)–S(1)–C(18)	98.4(4)	C(6′)–N(7)–C(8′)	114.1(11)	S(4)–C(5)–C(6)	105.6(7)	N(16)–C(17)–C(18)	110.2(7)
Pd–S(13)–C(12)	101.8(3)	C(6′)–N(7)–C(7N′)	119.1(12)	S(4)–C(5)–C(6′)	108.4(8)	N(16)–C(17′)–C(18)	108.6(18)
Pd–S(13)–C(14)	109.4(3)	C(8)–N(7)–C(7N)	115.6(9)	N(7)–C(6)–C(5)	108.5(9)	S(1)–C(18)–C(17)	106.6(6)
C(12)–S(13)–C(14)	98.0(4)	C(8′)–N(7)–C(7N′)	107.1(12)	N(7)–C(6′)–C(5)	107.4(12)	S(1)–C(18)–C(17′)	108.2(11)

C(18)–S(1)–C(2)–C(3)	−70.6(7)	C(7N′)–N(7)–C(8′)–C(9)	−168.1(13)
C(2)–S(1)–C(18)–C(17)	−150.8(6)	C(17)–N(16)–C(15)–C(14)	157.7(7)
C(2)–S(1)–C(18)–C(17′)	157.9(12)	C(16N)–N(16)–C(15)–C(14)	−76.2(10)
C(14)–S(13)–C(12)–C(11)	71.4(7)	C(17′)–N(16)–C(15′)–C(14)	57.9(22)
C(12)–S(13)–C(14)–C(15)	−161.7(6)	C(16′)–N(16)–C(15′)–C(14)	−172.2(20)
C(12)–S(13)–C(14)–C(15′)	146.5(11)	C(15)–N(16)–C(17)–C(18)	−67.2(9)
C(5)–S(4)–C(3)–C(2)	−67.1(7)	C(16N)–N(16)–C(17)–C(18)	163.4(8)
C(3)–S(4)–C(5)–C(6)	−148.2(7)	C(15′)–N(16)–C(17′)–C(18)	−158.8(16)
C(3)–S(4)–C(5)–C(6′)	159.8(9)	C(16′)–N(16)–C(17′)–C(18)	80.4(25)
C(11)–S(10)–C(9)–C(8)	−159.2(7)	S(1)–C(2)–C(3)–S(4)	−59.1(8)
C(11)–S(10)–C(9)–C(8′)	147.0(8)	S(4)–C(5)–C(6)–N(7)	−52.4(9)
C(9)–S(10)–C(11)–C(12)	70.8(7)	S(4)–C(5)–C(6′)–N(7)	46.6(12)
C(8)–N(7)–C(6)–C(5)	−66.2(10)	N(7)–C(8)–C(9)–S(10)	−45.2(9)
C(7N)–N(7)–C(6)–C(5)	166.7(9)	N(7)–C(8′)–C(9)–S(10)	60.0(11)
C(8′)–N(7)–C(6′)–C(5)	−158.6(11)	S(10)–C(11)–C(12)–S(13)	55.3(8)
C(7N′)–N(7)–C(6′)–C(5)	73.2(16)	S(13)–C(14)–C(15)–N(16)	−43.6(9)
C(6′)–N(7)–C(8)–C(9)	159.2(8)	S(13)–C(14)–C(15′)–N(16)	58.2(17)
C(7N′)–N(7)–C(8)–C(9)	−78.5(11)	N(16)–C(17)–C(18)–S(1)	−51.0(8)
C(6′)–N(7)–C(8′)–C(9)	57.8(15)	N(16)–C(17′)–C(18)–S(1)	48.3(18)

carried out using a double platinum electrode and a Ag–AgCl reference electrode. All potentials are quoted *versus* ferrocene–ferrocenium. *X*-Band e.s.r. spectra were recorded using a Bruker ER-200D spectrometer employing 100-kHz field modulation: all spectra were measured as glasses in MeCN at 77 K. Mass spectra were run by electron impact on a Kratos MS902 spectrometer and by f.a.b. on a Kratos MS50TC spectrometer. Proton and ^{13}C n.m.r. spectra were obtained on Bruker WP80, WP200, and WH360 instruments.

Synthesis of $[Pd(Me_2[18]aneN_2S_4)][PF_6]_2$.—Reaction of $PdCl_2$ (15 mg, 0.086 mmol) with $Me_2[18]aneN_2S_4$ (31 mg, 0.087 mmol) in refluxing MeCN–H_2O (3:1 v/v) under N_2 for 5 h afforded an orange solution. Addition of an excess of NH_4PF_6 and removal of the MeCN gave an orange precipitate, which was recrystallised from MeCN (yield: 40 mg, 63%) (Found: C, 21.7; H, 3.90; N, 3.75; S, 16.6%; *M*, 751.0. Calc. for $[C_{14}H_{30}N_2PdS_4][PF_6]_2$: C, 22.4; H, 4.05; N, 3.75; S, 17.1%). F.a.b. mass spectrum (3-nitrobenzyl alcohol matrix): *m/z* 604, 460; calc. for $[^{106}Pd(Me_2[18]aneN_2S_4)PF_6]^+$ and $[^{106}Pd(Me_2[18]aneN_2S_4)]^+$, 605 and 460 respectively. ^1H N.m.r. spectrum (80.13 MHz, CD_3CN, 298 K): δ 2.48 (s, CH_3, 6 H) and 2.68—3.50 (m, CH_2, 24 H). ^{13}C DEPT n.m.r. spectrum (50.32 MHz, CD_3CN, 298 K): δ 49.87 (CH_2N), 40.31 (SCH_2CH_2N), 39.40 (SCH_2CH_2S), and 41.57 p.p.m. (CH_3). U.v.–visible spectrum (MeCN): $\lambda_{max.}$ = 373 ($\varepsilon_{max.}$ = 3 000), 298 (14 460), and 232 nm (15 070 $dm^3\ mol^{-1}\ cm^{-1}$). I.r. spectrum (KBr disc): 2 950w, 2 850w, 1 420m, 1 400m, 1 370m, 1 300w, 1 260w, 1 240m, 1 210w, 1 150w, 1 120w, 1 110w, 1 060w, 1 005w, 940m, 840vs, 740m, 730w, 670w, and 555vs cm^{-1}.

Single Crystal Structure of $[Pd(Me_2[18]aneN_2S_4)][PF_6]_2 \cdot Me_2CO$.—Vapour diffusion of diethyl ether into a solution of the complex in Me_2CO gave crystals of diffraction quality. A yellow plate, 0.92 × 0.15 × 0.08 mm, was selected and mounted in a Lindemann glass capillary tube to prevent solvent loss.

Crystal data. $[C_{14}H_{30}N_2PdS_4][PF_6]_2 \cdot C_3H_6O$, *M* = 808.9, orthorhombic, space group *Pcab*, *a* = 14.336 9(15), *b* = 17.691 5(7), *c* = 24.295 2(11) Å, *U* = 6 162 $Å^3$ [from 2θ values of 58 reflections measured at ±ω (24 < 2θ < 25°, λ = 0.710 73 Å)], *Z* = 8, D_c = 1.744 g cm^{-3}, μ(Mo-K_α) = 1.044 mm^{-1}, *F*(000) = 3 264.

Data collection and processing. Stoë STADI-4 four-circle diffractometer, graphite-monochromated Mo-K_α radiation, ω—2θ scans using the learnt-profile method,[18] 4 527 reflections measured ($2\theta_{max.}$ = 45°, *h* 0—15, *k* 0—16, *l* 0—24) giving 2 693 with $F > 6\sigma(F)$. No significant crystal decay, no absorption correction.

Structure analysis and refinement. A Patterson synthesis located the Pd atom and the structure was developed by least-

Table 2. Fractional atomic co-ordinates with e.s.d.s for $[Pd(Me_2[18]aneN_2S_4)]^{2+}$

Atom	*x*	*y*	*z*	Atom	*x*	*y*	*z*
Pd	0.233 17(4)	0.114 56(3)	0.118 57(2)	C(16N)	0.045 3(10)	0.079 0(7)	−0.053 8(4)
S(1)	0.071 91(15)	0.095 74(11)	0.112 90(9)	C(16′)	−0.006 1(22)	0.093 1(24)	−0.035 9(17)
S(13)	0.253 06(15)	0.061 40(12)	0.031 89(8)	P(1)	0.520 03(18)	0.336 69(13)	0.379 54(9)
S(4)	0.212 76(17)	0.166 95(12)	0.205 87(8)	F(1)	0.056 6(5)	0.203 1(3)	0.433 18(21)
S(10)	0.393 49(15)	0.133 69(12)	0.123 31(9)	F(2)	−0.052 5(7)	0.118 4(4)	0.413 0(4)
N(7)	0.387 8(5)	0.105 1(4)	0.242 6(3)	F(3)	0.085 4(7)	0.210 7(5)	0.343 8(3)
N(16)	0.075 4(5)	0.120 7(3)	−0.004 97(25)	F(4)	−0.014 6(5)	0.123 7(3)	0.324 86(23)
C(2)	0.036 9(7)	0.114 2(6)	0.183 2(4)	F(5)	−0.051 7(7)	0.227 9(4)	0.373 3(3)
C(3)	0.087 9(7)	0.181 7(5)	0.207 0(4)	F(6)	0.086 9(7)	0.097 2(5)	0.387 1(3)
C(5)	0.220 5(6)	0.089 6(5)	0.256 4(4)	P(2)	0.232 14(18)	0.376 09(15)	0.108 16(13)
C(6)	0.315 0(7)	0.099 7(8)	0.285 0(5)	F(7)	0.294 0(7)	0.340 2(8)	0.153 7(5)
C(6′)	0.314 6(8)	0.047 4(7)	0.247 5(11)	F(8)	0.150 2(6)	0.324 3(6)	0.126 0(4)
C(8)	0.397 6(9)	0.034 3(5)	0.212 6(4)	F(9)	0.268 3(8)	0.315 6(8)	0.066 7(5)
C(8′)	0.473 4(9)	0.078 5(13)	0.214 3(6)	F(10)	0.316 4(7)	0.426 9(5)	0.093 9(7)
C(9)	0.445 4(6)	0.050 4(5)	0.156 7(3)	F(11)	0.196 5(8)	0.430 4(8)	0.154 2(6)
C(11)	0.430 1(6)	0.114 0(6)	0.053 2(4)	F(12)	0.170 1(7)	0.414 2(13)	0.066 3(7)
C(12)	0.378 8(6)	0.048 8(5)	0.029 1(3)	F(13)	0.189(3)	0.449 1(24)	0.112 5(23)
C(14)	0.243 1(6)	0.135 0(5)	−0.020 5(4)	F(14)	0.310(3)	0.400(3)	0.139 0(19)
C(15)	0.149 0(6)	0.175 5(5)	−0.014 2(5)	F(15)	0.286(4)	0.396(3)	0.051 7(19)
C(15′)	0.148 6(9)	0.118 2(24)	−0.047 5(7)	F(16)	0.279(3)	0.301 2(19)	0.101 0(15)
C(17)	−0.006 5(7)	0.153 7(6)	0.022 1(4)	F(17)	0.148(4)	0.353(3)	0.067 6(24)
C(17′)	0.068(3)	0.192 4(8)	0.025 4(9)	C(1S)	0.211 3(8)	0.390 3(6)	0.348 4(6)
C(18)	0.017 4(6)	0.177 1(5)	0.080 6(3)	C(2S)	0.212 1(9)	0.358 7(7)	0.404 2(5)
C(7N)	0.472 7(10)	0.132 6(10)	0.269 9(7)	C(3S)	0.234 9(9)	0.342 8(7)	0.301 8(5)
C(7N′)	0.417 8(20)	0.146 1(13)	0.291 9(7)	O(1S)	0.190 9(8)	0.454 3(5)	0.341 2(4)

squares refinement and difference Fourier synthesis to reveal all the other non-H atom positions.[19] It was discovered that one PF_6^- counter-ion and both –CN(Me)C– moieties were affected by disorder. This was modelled successfully using partial F and C atoms respectively, thus generating two alternative sites for the C atoms adjacent to the NMe functions and giving a total of six F atoms per P atom. The crystal lattice was found to contain one molecule of acetone per cation. Anisotropic thermal parameters were refined for Pd, S, P, N, O and all fully occupied C and F atoms. Hydrogen atoms were included in fixed, calculated positions.[19] The weighting scheme $w^{-1} = \sigma^2(F) + 0.000\,843F^2$ gave satisfactory agreement analyses. At convergence R, $R' = 0.0450$, 0.0606 respectively, $S = 1.186$ for 375 independent parameters, and the final difference Fourier synthesis showed no feature above 0.84 or below −0.50 e Å^{-3}. Bond lengths, angles and torsion angles appear in Table 1 and fractional atomic co-ordinates are given in Table 2.

Synthesis of $[Pt(Me_2[18]aneN_2S_4)][PF_6]_2$.—Reaction of $PtCl_2$ (30 mg, 0.113 mmol) with $Me_2[18]aneN_2S_4$ (40 mg, 0.113 mmol) under the same conditions as for the Pd analogue above gave a pale yellow product (yield: 55 mg, 58%) (Found: C, 19.7; H, 3.55, N, 3.35, S, 15.3%; *M*, 839.6. Calc. for $[C_{14}H_{30}N_2PtS_4][PF_6]_2$: C, 20.0; H, 3.60; N, 3.35, S, 15.3%). F.a.b. mass spectrum (3-nitrobenzyl alcohol matrix): *m/z* 694, 549; calc. for $[^{195}Pt(Me_2[18]aneN_2S_4)PF_6]^+$ and $[^{195}Pt(Me_2[18]aneN_2S_4)]^+$, 694 and 549 respectively. ^{1}H N.m.r. spectrum (200.13 MHz, CD_3CN, 298 K): δ 2.46 (s, CH_3, 6 H), 2.54—2.62 and 2.80—2.87 (m, NCH_2, 8 H), 3.18—3.30 and 3.55—3.62 (m, CH_2SCH_2, 16 H). ^{13}C DEPT n.m.r. spectrum (50.32 MHz, CD_3CN, 298 K): δ 49.18 (CH_2N), 39.87 (SCH_2CH_2N), 39.28 (SCH_2CH_2S), and 40.83 p.p.m. (CH_3). U.v.–visible spectrum (MeCN): $\lambda_{max.}$ = 243 nm ($\lambda_{max.}$ = 22 800 dm^3 mol^{-1} cm^{-1}). I.r. spectrum (KBr disc): 2 950m, 2 920w, 2 840w, 1 460m, 1 420m, 1 379w, 1 310m, 1 260w, 1 240w, 1 220w, 1 110m, 1 070m, 1 030w, 1 015w, 980w, 840vs, 745m, 555vs, and 340m cm^{-1}.

Synthesis of $[Pd([18]aneN_2S_4)][PF_6]_2$.—To a refluxing solution of $[18]aneN_2S_4$ (47 mg, 0.144 mmol) in MeCN (30 cm^3) was added $PdCl_2$ (25 mg, 0.141 mmol) and $TlPF_6$ (110 mg, 0.310 mmol). The reaction mixture was refluxed for 3 h under N_2 to yield a purple solution and a fine white precipitate. After cooling, the white precipitate of TlCl was removed by filtration to leave a purple solution. Removal of the solvent and recrystallisation from H_2O afforded a dark blue product (yield: 50 mg, 49%) (Found: C, 19.3; H, 3.60; N, 3.85; S, 17.8%; *M*, 722.9. Calc. for $[C_{12}H_{26}N_2PdS_4][PF_6]_2$: C, 19.9; H, 3.60, N, 3.90; S, 17.7%). F.a.b. mass spectrum (3-nitrobenzyl alcohol matrix): *m/z* 577, 431; calc. for $[^{106}Pd([18]aneN_2S_4)PF_6]^+$ and $[^{106}Pd([18]aneN_2S_4)]^+$, 577 and 432 respectively. ^{1}H N.m.r. spectrum [360.13 MHz, $(CD_3)_2CO$, 298 K]: δ 3.7—2.56 (br, CH_2) and 5.0 p.p.m. (br, NH). ^{13}C DEPT n.m.r. spectrum (50.32 MHz, CD_3CN, 298 K): resonances very broad, not easily distinguished from noise. Only slightly better resolved at 90.56 MHz [298 K in $(CD_3)_2CO$]: δ 56.28, 51.12, 47.26, 34.05, 31.88, and 27.29 p.p.m. (CH_2). U.v.–visible spectrum (MeCN): $\lambda_{max.}$ = 514 ($\varepsilon_{max.}$ = 124), 322 (2 815), 266 (9 420), and 233 nm (12 140 dm^3 mol^{-1} cm^{-1}). I.r. spectrum (KBr disc): 3 260m, 3 120m, 3 000w, 2 930m, 1 460m, 1 425m, 1 300m, 1 270w, 1 230m, 1 210w, 1 150w, 1 130w, 1 105m, 1 060w, 1 030w, 1 015w, 1 000w, 980w, 840vs, 740m, 640w, and 555vs cm^{-1}.

Single Crystal Structure of $[Pd([18]aneN_2S_4)][BPh_4]_2$.—Single crystals suitable for *X*-ray crystallography were obtained by metathesis of $[Pd([18]aneN_2S_4)][PF_6]_2$ with $NaBPh_4$ in H_2O, which yielded a green precipitate. Recrystallisation from $MeNO_2$ afforded green columnar crystals. A single crystal (0.30 × 0.10 × 0.08 mm) was selected and sealed in a Lindemann glass capillary tube to prevent solvent loss.

Crystal data. $[C_{12}H_{26}N_2PdS_4][C_{24}H_{20}B]_2$, M = 1 071.5, monoclinic, space group $P2_1/c$, a = 16.888 8(12), b = 16.553 3(15), c = 18.537 6(12) Å, β = 93.144(8)°, U = 5 174.6 Å^3 [from 2θ values for 36 reflections measured at ±ω (15 < 2θ < 17°, λ = 0.710 73 Å)], Z = 4, D_c = 1.375 g cm^{-3}, μ(Mo-K_α) = 0.548 mm^{-1}, F(000) = 2 240.

Data collection and processing. Stoë STADI-4 four-circle diffractometer, graphite-monochromated Mo-K_α radiation,

Table 3. Bond lengths (Å), angles and torsion angles (°) with e.s.d.s for $[Pd([18]aneN_2S_4)]^{2+}$

Pd–S(1)	2.311(3)	S(13)–C(12)	1.815(14)
Pd–S(4)	3.000(3)	S(13)–C(14)	1.810(11)
Pd–S(10)	2.954(4)	N(7)–C(6)	1.472(12)
Pd–S(13)	2.357(3)	N(7)–C(8)	1.481(12)
Pd–N(7)	2.123(7)	N(16)–C(15)	1.487(13)
Pd–N(16)	2.068(7)	N(16)–C(17)	1.463(14)
S(1)–C(2)	1.778(11)	C(2)–C(3)	1.545(16)
S(1)–C(18)	1.835(12)	C(5)–C(6)	1.523(14)
S(4)–C(3)	1.798(12)	C(8)–C(9)	1.512(15)
S(4)–C(5)	1.806(11)	C(11)–C(12)	1.493(20)
S(10)–C(9)	1.795(12)	C(14)–C(15)	1.506(16)
S(10)–C(11)	1.788(15)	C(17)–C(18)	1.497(16)
S(1)–Pd–S(4)	81.55(9)	C(9)–S(10)–C(11)	104.2(6)
S(1)–Pd–S(10)	101.52(10)	Pd–S(13)–C(12)	110.6(4)
S(1)–Pd–S(13)	169.54(10)	Pd–S(13)–C(14)	98.5(4)
S(1)–Pd–N(7)	93.93(19)	C(12)–S(13)–C(14)	102.8(6)
S(1)–Pd–N(16)	85.16(21)	Pd–N(7)–C(6)	112.7(5)
S(4)–Pd–S(10)	158.94(9)	Pd–N(7)–C(8)	115.0(5)
S(4)–Pd–S(13)	100.05(9)	C(6)–N(7)–C(8)	108.7(7)
S(4)–Pd–N(7)	78.68(19)	Pd–N(16)–C(15)	109.4(6)
S(4)–Pd–N(16)	101.29(20)	Pd–N(16)–C(17)	112.1(6)
S(10)–Pd–S(13)	80.75(9)	C(15)–N(16)–C(17)	113.2(8)
S(10)–Pd–N(7)	80.31(19)	S(1)–C(2)–C(3)	118.7(8)
S(10)–Pd–N(16)	99.73(21)	S(4)–C(3)–C(2)	117.9(8)
S(13)–Pd–N(7)	96.51(19)	S(4)–C(5)–C(6)	115.8(7)
S(13)–Pd–N(16)	84.39(21)	N(7)–C(6)–C(5)	114.3(8)
N(7)–Pd–N(16)	179.1(3)	N(7)–C(8)–C(9)	114.3(8)
Pd–S(1)–C(2)	110.5(4)	S(10)–C(9)–C(8)	119.4(8)
Pd–S(1)–C(18)	97.0(4)	S(10)–C(11)–C(12)	120.7(10)
C(2)–S(1)–C(18)	101.6(5)	S(13)–C(12)–C(11)	118.2(10)
Pd–S(4)–C(3)	94.8(4)	S(13)–C(14)–C(15)	111.3(8)
Pd–S(4)–C(5)	87.4(3)	N(16)–C(15)–C(14)	110.2(9)
C(3)–S(4)–C(5)	101.6(5)	N(16)–C(17)–C(18)	108.6(9)
Pd–S(10)–C(9)	86.7(4)	S(1)–C(18)–C(17)	105.8(8)
Pd–S(10)–C(11)	96.9(5)		

C(18)–S(1)–C(2)–C(3)	61.4(9)
C(2)–S(1)–C(18)–C(17)	−153.2(8)
C(5)–S(4)–C(3)–C(2)	59.1(9)
C(3)–S(4)–C(5)–C(6)	−123.1(8)
C(11)–S(10)–C(9)–C(8)	−65.7(10)
C(9)–S(10)–C(11)–C(12)	63.2(12)
C(14)–S(13)–C(12)–C(11)	67.4(11)
C(12)–S(13)–C(14)–C(15)	−94.8(9)
C(8)–N(7)–C(6)–C(5)	168.9(8)
C(6)–N(7)–C(8)–C(9)	179.6(8)
C(17)–N(16)–C(15)–C(14)	−176.7(9)
C(15)–N(16)–C(17)–C(18)	−176.6(9)
S(1)–C(2)–C(3)–S(4)	50.5(11)
S(4)–C(5)–C(6)–N(7)	63.8(10)
N(7)–C(8)–C(9)–S(10)	−59.2(11)
S(10)–C(11)–C(12)–S(13)	44.0(15)
S(13)–C(14)–C(15)–N(16)	−49.3(10)
N(16)–C(17)–C(18)–S(1)	62.0(10)

ω—2θ scans using the learnt-profile method,[18] 6 815 reflections measured ($2\theta_{max.}$ = 45°, h −18 to 14, k 0—17, l 0—19), giving 4 006 with $F > 4\sigma(F)$. No significant crystal decay, no absorption correction.

Structure analysis and refinement. A Patterson synthesis located the Pd atom and this was input to DIRDIF[20] which identified the positions of all non-H atoms except for one macrocyclic C atom. The structure was developed by least-squares refinement and difference Fourier synthesis.[19] Anisotropic thermal parameters were refined for Pd, S, N, C, and B atoms. Hydrogen atoms were included in fixed, calculated positions.[19] The weighting scheme $w^{-1} = \sigma^2(F) + 0.001\,155F^2$ gave satisfactory agreement analyses. At convergence R, R' = 0.0623, 0.0786 respectively, S = 1.110 for 517 independent parameters, and the final difference Fourier synthesis showed no feature above 0.48 or below −0.45 e Å^{-3}. Bond lengths, angles and torsion angles are given in Table 3 and fractional atomic coordinates are given in Table 4.

Synthesis of $[Pt([18]aneN_2S_4)][PF_6]_2$.—Method as for the Pd analogue above using $PtCl_2$ (33 mg, 0.123 mmol), $TlPF_6$ (103 mg, 0.294 mmol), and $[18]aneN_2S_4$ (40 mg, 0.123 mmol). The product was isolated as a yellow solid (yield: 80 mg, 81%) (Found: C, 17.1; H, 3.10, N, 3.45; S, 15.5%; M, 811.5. Calc. for $[C_{12}H_{26}N_2PtS_4][PF_6]_2$: C, 17.8; H, 3.25, N, 3.45; S, 15.8%). F.a.b. mass spectrum (3-nitrobenzyl alcohol matrix): m/z 667, 521; calc. for $[^{195}Pt([18]aneN_2S_4)PF_6]^+$ and $[^{195}Pt([18]aneN_2S_4)]^+$, 666 and 521 respectively. ^1H N.m.r. spectrum (360.13 MHz, CD_3CN, 298 K): δ 5.68 (br, NH, 1 H), 3.76 (br NH, 1 H), 3.42—2.84 (br, CH_2, 24 H). ^{13}C DEPT n.m.r. spectrum [50.32 MHz, $(CD_3)_2CO$, 298 K]: δ 28.08, 34.74, 36.84, 53.11, and 55.39 p.p.m. (CH_2). ^{13}C DEPT n.m.r. spectrum [90.56 MHz, $(CD_3)_2CO$ 298 K]: δ 56.1 (NCH_2, 2 C), 53.8 (NCH_2, 2 C), 46.6, 42.0, 38.3, 37.3, 35.3 (two overlapping resonances), 28.2, and 26.3 p.p.m. (SCH_2, total of 8 C). I.r. spectrum (KBr disc): 3 140m, 3 000w, 2 945w, 1 460m, 1 420m, 1 410m, 1 310m, 1 270w, 1 240w, 1 220w, 1 125m, 1 055m, 1 020m, 840vs, 720m, and 555vs cm^{-1}.

Synthesis of $[Pd_2Cl_2([18]aneN_2S_4)][PF_6]_2$.—Reaction of $PdCl_2$ (44 mg, 0.245 mmol) with $[18]aneN_2S_4$ (40 mg, 0.123 mmol) in refluxing MeCN–H_2O (1:1 v/v) for 4 h under N_2 afforded a yellow solution. Addition of an excess of NH_4PF_6 gave a yellow precipitate which was recrystallised from MeCN to yield the product as yellow needles (yield 105 mg, 95%) (Found: C, 15.9; H, 2.80, N, 3.30; S, 14.4%; M, 900.2. Calc. for $[C_{12}H_{26}Cl_2N_2Pd_2S_4][PF_6]_2$: C, 16.0; H, 2.90; N, 3.10; S, 14.2%). F.a.b. mass spectrum (3-nitrobenzyl alcohol matrix): m/z 609, 575, 539, 431; calc. for $[^{106}Pd_2{}^{35}Cl_2([18]aneN_2S_4)]^+$, $[^{106}Pd_2{}^{35}Cl([18]aneN_2S_4)]^+$, $[^{106}Pd_2([18]aneN_2S_4)]^+$, $[^{106}Pd([18]aneN_2S_4)]^+$, 608, 573, 538, and 432 respectively. ^1H N.m.r. spectrum (80.13 MHz, CD_3CN, 298 K): δ 2.7—3.6 and 4.2—4.6 (m, CH_2, 24 H), 5.6 (br, NH, 2 H). ^{13}C DEPT n.m.r. spectrum (50.32 MHz, CD_3CN. 298 K): δ 54.77 (NCH_2, 4 C), 38.28 (NCH_2CH_2S, 4 C), and 30.44 p.p.m. (SCH_2CH_2S, 4 C). U.v.–visible spectrum (MeCN): $\lambda_{max.}$ = 376 ($\varepsilon_{max.}$ = 3 540), 262, (17 330), and 224 nm (22 200 dm^3 mol^{-1} cm^{-1}). I.r. spectrum (KBr disc): 3 200m, 3 060m, 3 000w, 2 965w, 1 460m, 1 420vs, 1 330w, 1 310m, 1 270w, 1 260m, 1 225w, 1 140w, 1 120w, 1 100m, 1 060m, 1 010m, 840vs, 740m, 650w, 555vs, and 330m cm^{-1}.

Single Crystal Structure of $[Pd_2Cl_2([18]aneN_2S_4)][PF_6]_2 \cdot 2MeCN$.—Recrystallisation of the complex from MeCN afforded yellow needles of diffraction quality. A suitable crystal (0.77 × 0.23 × 0.19 mm) was selected and sealed in a Lindemann glass capillary tube to prevent solvent loss.

Crystal data. $[C_{12}H_{26}Cl_2N_2Pd_2S_4][PF_6]_2 \cdot 2CH_3CN$, M = 982.2, monoclinic, space group $C2/c$, a = 18.617(13), b = 15.569(11), c = 14.323(14) Å, β = 113.59(5)°, U = 3 804.6 Å^3 [from 2θ values of 32 reflections measured at ±ω (24 < 2θ < 25°, λ = 0.710 73 Å)], Z = 4, D_c = 1.715 g cm^{-3}, μ(Mo-K_α) = 1.443 mm^{-1}, F(000) = 1 936.

Data collection and processing. Stoë STADI-4 four-circle diffractometer, graphite-monochromated Mo-K_α radiation, ω—2θ scans, 2 456 reflections measured ($2\theta_{max.}$ = 45°, h −20 to 18, k 0—16, l 0—15) giving 1 708 with $F > 6\sigma(F)$. No significant crystal decay was observed.

Structure analysis and refinement. A Patterson synthesis located the Pd atom and the structure was developed by least-squares refinement and difference Fourier synthesis to reveal all the other non-H atom positions.[19] Absorption corrections (min.,

Table 4. Fractional atomic co-ordinates with e.s.d.s for $[Pd([18]aneN_2S_4)]^{2+}$*

Atom	*x*	*y*	*z*
Pd	0.255 62(4)	0.006 74(4)	0.242 57(3)
S(1)	0.291 33(16)	0.141 33(15)	0.250 85(14)
S(4)	0.095 85(16)	0.076 26(18)	0.269 44(15)
S(10)	0.409 76(18)	−0.074 05(23)	0.273 08(18)
S(13)	0.219 05(17)	−0.126 67(15)	0.211 20(14)
N(7)	0.251 8(4)	0.008 2(4)	0.356 1(3)
N(16)	0.260 1(4)	0.023 1(4)	0.132 3(4)
C(2)	0.215 1(7)	0.198 7(6)	0.289 1(6)
C(3)	0.127 8(7)	0.179 7(6)	0.265 9(6)
C(5)	0.116 0(6)	0.052 5(6)	0.363 8(5)
C(6)	0.170 6(5)	−0.019 2(6)	0.379 5(5)
C(8)	0.302 4(6)	−0.074 1(6)	0.387 1(5)
C(9)	0.387 8(7)	−0.070 4(7)	0.366 7(5)
C(11)	0.379 1(10)	−0.172 9(9)	0.244 4(7)
C(12)	0.294 1(10)	−0.197 6(7)	0.245 2(6)
C(14)	0.236 0(7)	−0.122 1(7)	0.115 7(5)
C(15)	0.289 0(7)	−0.052 2(8)	0.098 8(5)
C(17)	0.306 2(7)	0.094 6(8)	0.114 6(6)
C(18)	0.275 3(7)	0.165 5(7)	0.154 5(6)
C(1R)	0.488 7(3)	0.198 5(3)	1.006 90(23)
C(2R)	0.524 5(3)	0.125 3(3)	0.990 30(23)
C(3R)	0.550 4(3)	0.072 9(3)	1.045 60(23)
C(4R)	0.540 5(3)	0.093 6(3)	1.117 49(23)
C(5R)	0.504 7(3)	0.166 8(3)	1.134 08(23)
C(6R)	0.478 8(3)	0.219 2(3)	1.078 80(23)
C(7R)	0.393 7(3)	0.327 3(3)	0.967 9(3)
C(8R)	0.313 0(3)	0.311 5(3)	0.972 1(3)
C(9R)	0.264 9(3)	0.366 2(3)	1.006 6(3)
C(10R)	0.297 5(3)	0.436 7(3)	1.036 8(3)
C(11R)	0.378 3(3)	0.452 5(3)	1.032 6(3)
C(12R)	0.426 4(3)	0.397 8(3)	0.998 2(3)
C(13R)	0.410 7(3)	0.196 7(3)	0.874 55(25)
C(14R)	0.358 2(3)	0.139 1(3)	0.898 89(25)
C(15R)	0.318 6(3)	0.087 3(3)	0.849 73(25)
C(16R)	0.331 6(3)	0.093 1(3)	0.776 25(25)
C(17R)	0.384 1(3)	0.150 8(3)	0.751 91(25)
C(18R)	0.423 7(3)	0.202 6(3)	0.801 06(25)
C(19R)	0.535 2(3)	0.307 1(3)	0.904 1(3)
C(20R)	0.612 2(3)	0.293 2(3)	0.932 4(3)
C(21R)	0.675 7(3)	0.334 8(3)	0.904 7(3)
C(22R)	0.662 1(3)	0.390 3(3)	0.848 7(3)
C(23R)	0.585 1(3)	0.404 2(3)	0.820 4(3)
C(24R)	0.521 6(3)	0.362 6(3)	0.848 1(3)
C(25R)	1.017 8(4)	0.201 8(3)	0.633 9(3)
C(26R)	1.095 5(4)	0.176 0(3)	0.626 3(3)
C(27R)	1.132 6(4)	0.126 2(3)	0.678 6(3)
C(28R)	1.092 0(4)	0.102 2(3)	0.738 5(3)
C(29R)	1.014 3(4)	0.128 0(3)	0.746 2(3)
C(30R)	0.977 2(4)	0.177 8(3)	0.693 9(3)
C(31R)	0.889 8(3)	0.299 7(4)	0.596 5(3)
C(32R)	0.817 1(3)	0.286 1(4)	0.559 0(3)
C(33R)	0.748 1(3)	0.320 5(4)	0.583 6(3)
C(34R)	0.751 8(3)	0.368 3(4)	0.645 6(3)
C(35R)	0.824 5(3)	0.381 8(4)	0.683 1(3)
C(36R)	0.893 5(3)	0.347 5(4)	0.658 6(3)
C(37R)	0.951 4(3)	0.198 9(3)	0.495 91(25)
C(38R)	0.945 7(3)	0.115 4(3)	0.504 27(25)
C(39R)	0.922 3(3)	0.067 0(3)	0.445 24(25)
C(40R)	0.904 7(3)	0.102 2(3)	0.377 87(25)
C(41R)	0.910 4(3)	0.185 7(3)	0.369 52(25)
C(42R)	0.933 8(3)	0.234 0(3)	0.428 53(25)
C(43R)	1.039 0(4)	0.330 5(4)	0.542 4(4)
C(44R)	1.092 2(4)	0.310 7(4)	0.490 1(4)
C(45R)	1.141 0(4)	0.370 1(4)	0.463 0(4)
C(46R)	1.136 7(4)	0.449 4(4)	0.488 1(4)
C(47R)	1.083 5(4)	0.469 2(4)	0.540 3(4)
C(48R)	1.034 7(4)	0.409 8(4)	0.567 4(4)
B(1)	0.456 9(6)	0.256 0(6)	0.935 9(5)
B(2)	0.974 2(7)	0.258 3(7)	0.568 9(6)

* R indicates carbon atoms of BPh_4^- anions.

Table 5. Bond lengths (Å), angles and torsion angles (°) with e.s.d.s for $[Pd_2Cl_2([18]aneN_2S_4)]^{2+}$

Pd–Cl(1)	2.305(4)	C(3)–N(4)	1.549(20)
Pd–S(1)	2.317(4)	N(4)–C(5)	1.479(21)
Pd–N(4)	2.049(13)	C(5)–C(6)	1.486(24)
Pd–S(7)	2.316(4)	C(6)–S(7)	1.847(18)
S(1)–C(2)	1.819(17)	C(17)–C(18)	1.509(22)
S(1)–C(18)	1.815(16)	C(17)–S(7′)	1.856(16)
C(2)–C(3)	1.525(23)		
Cl(1)–Pd–S(1)	93.16(14)	C(2)–C(3)–N(4)	106.6(12)
Cl(1)–Pd–N(4)	178.8(4)	Pd–N(4)–C(3)	110.7(9)
Cl(1)–Pd–S(7)	93.38(14)	Pd–N(4)–C(5)	112.8(10)
S(1)–Pd–N(4)	87.4(4)	C(3)–N(4)–C(5)	112.3(12)
S(1)–Pd–S(7)	173.41(15)	N(4)–C(5)–C(6)	109.1(13)
N(4)–Pd–S(7)	86.1(4)	C(5)–C(6)–S(7)	111.1(12)
Pd–S(1)–C(2)	97.1(6)	Pd–S(7)–C(6)	97.2(6)
Pd–S(1)–C(18)	106.5(5)	C(18)–C(17)–S(7′)	108.5(10)
C(2)–S(1)–C(18)	100.3(7)	S(1)–C(18)–C(17)	108.5(10)
S(1)–C(2)–C(3)	111.3(11)	C(17)–S(7′)–C(6′)	99.3(8)
C(18)–S(1)–C(2)–C(3)	76.3(12)		
C(2)–S(1)–C(18)–C(17)	178.2(11)		
S(1)–C(2)–C(3)–C(4)	55.6(14)		
C(2)–C(3)–N(4)–C(5)	−179.5(12)		
C(3)–N(4)–C(5)–C(6)	177.3(13)		
N(4)–C(5)–C(6)–S(7)	−52.1(16)		
S(7′)–C(17)–C(18)–S(1)	147.9(8)		
C(18)–C(17)–S(7′)–C(6′)	178.6(11)		
C(17)–S(7′)–C(6′)–C(5′)	76.9(13)		

0.744; max., 1.463) were made using DIFABS.[21] During refinement some disorder of the PF_6^- counter-ion was identified. This was modelled successfully using partial F atoms, giving a total of six F atoms per P atom. Each binuclear cation was found to have two molecules of MeCN solvent associated. These too were found to be disordered, and were modelled by constraining the C–C and C–N bond lengths to be 1.50 and 1.23 Å respectively, and constraining the N–C–C angle to be linear.[19] Anisotropic thermal parameters were refined for Pd, Cl, S, P, F, N, and C atoms except for those associated with the solvent molecules. Hydrogen atoms were included in fixed, calculated positions. The weighting scheme $w^{-1} = \sigma^2(F) + 0.002\,282F^2$ gave satisfactory agreement analyses. At convergence $R, R' = 0.0757, 0.1037$ respectively, $S = 1.201$ for 177 independent parameters, and the final difference Fourier synthesis showed no feature above 0.97 or below −1.22 e Å^{-3}. Bond lengths, angles and torsion angles are given in Table 5 and fractional atomic co-ordinates in Table 6. Illustrations were prepared using ORTEP,[22] molecular geometry calculations utilised CALC,[23] and scattering factor data were taken from ref. 24.

Additional material available from the Cambridge Crystallographic data centre comprises thermal parameters and H-atom co-ordinates.

Synthesis of $[Pt_2Cl_2([18]aneN_2S_4)][PF_6]_2$.—Method as for the Pd analogue above, using $PtCl_2$ (65 mg, 0.246 mmol) and $[18]aneN_2S_4$ (40 mg, 0.123 mmol). The product was isolated as a pale yellow solid (yield: 73 mg, 55%) (Found: C, 13.8; H, 2.40. N, 2.85%; *M*, 1 077.42. Calc. for $[C_{12}H_{26}Cl_2N_2Pt_2S_4][PF_6]_2$:

Table 6. Fractional atomic co-ordinates with e.s.d.s for $[Pd_2Cl_2([18]aneN_2S_4)]^{2+}$

Atom	*x*	*y*	*z*
Pd	0.036 42(6)	0.012 22(6)	0.379 66(8)
Cl(1)	−0.094 63(20)	−0.019 77(22)	0.329 3(3)
S(1)	0.015 07(22)	0.158 98(23)	0.376 2(3)
C(2)	0.115 6(9)	0.192 2(10)	0.407 1(12)
C(3)	0.174 0(8)	0.127 3(9)	0.476 4(12)
N(4)	0.152 9(7)	0.039 7(7)	0.421 5(9)
C(5)	0.204 9(8)	−0.030 6(11)	0.481 3(12)
C(6)	0.178 6(9)	−0.112 7(11)	0.425 4(14)
S(7)	0.073 07(23)	−0.130 79(23)	0.391 2(3)
C(17)	−0.076 5(9)	0.164 4(10)	0.485 3(11)
C(18)	0.006 0(9)	0.185 5(9)	0.494 3(10)
P(1)	0.289 7(3)	0.179 5(4)	0.286 1(4)
F(1)	0.280 0(9)	0.234 0(11)	0.372 6(12)
F(2)	0.298 9(12)	0.120 0(12)	0.207 5(14)
F(3)	0.371 8(11)	0.148 5(13)	0.345 4(16)
F(4)	0.218 6(22)	0.125(3)	0.264(3)
F(5)	0.341 1(12)	0.250 3(15)	0.278 2(16)
F(6)	0.205(3)	0.262(4)	0.198(4)
F(7)	0.196 9(13)	0.189 6(17)	0.241 5(18)
F(8)	0.254 1(17)	0.227 9(19)	0.180 5(21)
F(9)	0.267 7(13)	0.092 3(15)	0.330 5(18)
F(10)	0.338 5(22)	0.153 6(24)	0.396(3)
N(1S)	0.387 7(16)	0.138 6(23)	0.032 9(20)
C(2S)	0.425 8(13)	0.138(3)	0.125 8(20)
C(3S)	0.477 4(20)	0.130 4(22)	0.237 1(21)

C, 13.4; H, 2.45; N, 2.60%). F.a.b. mass spectrum (dimethylformamide–glycerol matrix): *m/z* 786, 750, 555, 521; calc. for $[^{195}Pt_2{}^{35}Cl_2([18]aneN_2S_4)]^+$, $[^{195}Pt_2{}^{35}Cl([18]aneN_2S_4)]^+$, $[^{195}Pt^{35}Cl([18]aneN_2S_4)]^+$, $[^{195}Pt([18]aneN_2S_4)]^+$, 786, 751, 556, and 521 respectively. ^1H N.m.r. spectrum (80.13 MHz, CD_3CN, 298 K): δ 7.45 (br, NH) and 2.2—3.6 (m, CH_2). I.r. spectrum (KBr disc): 3 140m, 3 000w, 2 950w, 1 460m, 1 420m, 1 410m, 1 310m, 1 270w, 1 240w, 1 220w, 1 120m, 1 055w, 1 020m, 1 000w, 840vs, 740m, 555vs, and 330w cm^{-1}.

Acknowledgements

We thank the S.E.R.C. for support and Johnson Matthey plc for generous loans of platinum metals.

References

1 A. J. Blake and M. Schröder, *Adv. Inorg. Chem.*, 1990, **35**, 1.
2 M. Schröder, *Pure Appl. Chem.*, 1988, **60**, 517.
3 A. J. Blake, A. J. Holder, T. I. Hyde, and M. Schröder, *J. Chem. Soc., Chem. Commun.*, 1987, 987; A. J. Blake, A. J. Holder, T. I. Hyde, Y. V. Roberts, A. J. Lavery, and M. Schröder, *J. Organomet. Chem.*, 1987, **323**, 261.
4 A. J. Blake, L. M. Gordon, A. J. Holder, T. I. Hyde, G. Reid, and M. Schröder, *J. Chem. Soc., Chem. Commun.*, 1988, 1452; A. McAuley, T. W. Whitcombe, and G. Hunter, *Inorg. Chem.*, 1988, **27**, 2634; A. McAuley and T. W. Whitcombe, *ibid.*, p. 3090.
5 A. J. Blake, R. O. Gould, A. J. Holder, T. I. Hyde, M. O. Odulate, A. J. Lavery, and M. Schröder, *J. Chem. Soc., Chem. Commun.*, 1987, 118; J. D. Woollins and P. F. Kelly, *Coord. Chem. Rev.*, 1985, **65**, 115; T. V. O'Halloran and S. J. Lippard, *Isr. J. Chem.*, 1985, **25**, 130; R. Usón, J. Forniés, M. Thomás, B. Menjón, R. Bau, K. Sünkel, and E. Kuwabara, *Organometallics*, 1986, **5**, 1576; E. Bothe and R. K. Broszkiewicz, *Inorg. Chem.*, 1989, **28**, 2988 and refs. therein.
6 A. J. Blake, R. O. Gould, T. I. Hyde, and M. Schröder, *J. Chem. Soc., Chem. Commun.*, 1987, 431.
7 A. J. Blake, R. O. Gould, T. I. Hyde, and M. Schröder, *J. Chem. Soc., Chem. Commun.*, 1987, 1730.
8 D. St. C. Black and I. A. McLean, *Chem. Commun.*, 1968, 1004; *Tetrahedron Lett.*, 1969, 3961; *Aust. J. Chem.*, 1971, **24**, 1401.
9 B. Dietrich, J-M. Lehn, and J-P. Sauvage, *Chem. Commun.*, 1970, 1055; A. A. Alberts, R. Annunziata, and J-M. Lehn, *J. Am. Chem. Soc.*, 1977, **99**, 8502.
10 G. Reid, A. J. Blake, T. I. Hyde, and M. Schröder, *J. Chem. Soc., Chem. Commun.*, 1988, 1397.
11 A. J. Blake, R. O. Gould, A. J. Lavery, and M. Schröder, *Angew. Chem.*, 1986, **98**, 282; *Angew. Chem. Int. Ed. Engl.*, 1986, **25**, 274.
12 K. Broadley, G. A. Lane, N. G. Connelly, and W. E. Geiger, *J. Am. Chem. Soc.*, 1983, **105**, 2486; E. P. Talsi, V. P. Babenko, V. A. Likholobov, V. M. Nekipelov, and V. D. Chinakov, *J. Chem. Soc., Chem. Commun.*, 1985, 1768; P. Arrizabalaga, G. Bernardinelli, M. Geoffroy, P. Castan, and F. Dahan, *Chem. Phys. Lett.*, 1986, **124**, 549; G. A. Lane, W. E. Geiger, and N. G. Connelly, *J. Am. Chem. Soc.*, 1987, **109**, 402 and refs. therein.
13 R. C. Eachus and R. E. Groves, *J. Chem. Phys.*, 1976, **65**, 5445; R. Kirmse, J. Stach, W. Dietzsch, G. Steimecke, and E. Hoyer, *Inorg. Chem.*, 1980, **19**, 2679; A. Tressaud, S. Khairoun, J-M. Dance, J. Grannec, G. Demazeau, and P. Hagenmuller, *C. R. Acad. Sci., Paris Ser. II*, 1982, **295**, 183.
14 D. Parker, J. M. Lehn, and J. Rimmer, *J. Chem. Soc., Dalton Trans.*, 1985, 1517.
15 See, for example, 'Comprehensive Co-ordination Chemistry,' Pergamon, Oxford, 1987, vol. 5, ch. 51.
16 A. J. Blake, R. O. Gould, A. J. Holder, T. I. Hyde, A. J. Lavery, G. Reid, and M. Schröder, unpublished work.
17 C. O. Dietrich-Buchecker, J. M. Kern, and J. P. Sauvage, *J. Chem. Soc., Chem. Commun.*, 1985, 760.
18 W. Clegg, *Acta Crystallogr., Sect. A*, 1981, **37**, 22.
19 SHELX 76, program for crystal structure refinement, G. M. Sheldrick, University of Cambridge, 1976.
20 DIRDIF, Applications of Direct Methods to Difference Structure Factors, P. T. Beurskens, W. P. Bosman, H. M. Doesbury, Th. E. M. van den Hark, P. A. J. Prick, J. H. Noordik, G. Beurskens, R. O. Gould and V. Parthasarathia, University of Nijmegen, Netherlands, 1983.
21 DIFABS, program for empirical absorption corrections, N. Walker and D. Stuart, *Acta Crystallogr., Sect. A*, 1983, **39**, 158.
22 ORTEP II, interactive version, P. D. Mallinson and K. W. Muir, *J. Appl. Crystallogr.*, 1985, **18**, 51.
23 CALC, Fortran 77 version, R. O. Gould and P. Taylor, University of Edinburgh, 1985.
24 D. T. Cromer and J. L. Mann, *Acta Crystallogr., Sect. A*, 1968, **24**, 321.

Received 10*th May* 1990; *Paper* 0/02062A